ChemComm

COMMUNICATION

View Article Online
View Journal | View Issue

Cite this: *Chem. Commun.*, 2022, 58, 2754

Received 9th December 2021,
Accepted 28th January 2022

DOI: 10.1039/d1cc06950k

rsc.li/chemcomm

Switching photorelease to singlet oxygen generation by oxygen functionalization of phenothiazine photocages†

Mamata Ojha,[a] Moumita Banerjee,[b] Souvik Ray,[a] Amit Kumar Singh,[a] Anakuthil Anoop *[b] and N. D. Pradeep Singh *[a]

A phenothiazine-based photoremovable protecting group (PRPG) for single and dual release of carboxylic acids was developed. The change in the oxidation state of the sulfur atom of the phenothiazine PRPG resulted in singlet oxygen generation, rather than photorelease. The difference in the photochemistry between oxygen-free and oxygen-functionalized phenothiazine was investigated and supported by DFT calculations.

Photoremovable protecting groups (PRPGs) are used to achieve non-invasive spatiotemporal control over the release of biologically active molecules on exposure to light.[1] For this reason, PRPGs have gained considerable importance, particularly in drug delivery systems (DDSs).[2,3] At present, the applications of PRPGs are no longer restricted to the release of a single bioactive molecule of interest. PRPGs with dual release ability have become more important than those with single release ability in drug delivery as they reduce drug resistance,[4] therapeutic doses,[5] and side effects. In the literature, a few PRPGs for the dual release of active molecules are reported, including carboline,[6] carbazole,[7] *o*-nitrobenzyl,[8] and bimane[9] derivatives. Hence, there is a real need to develop a fluorescent PRPG for the dual release of the active molecules with moderate to high photochemical quantum yield in the visible wavelength region.

Phenothiazine (PTZ) is an active component in push–pull systems because of its strong electron-donating ability. The literature shows that the photophysical properties and the HOMO–LUMO energy levels of PTZ derivatives could be modulated by having substituents at the nitrogen and the 3,7-positions of the phenothiazine unit.[10] PTZ and its derivatives are used in various applications, from pharmacological to biological fields. Phenothiazine derivatives have gained considerable importance among nitrogen-containing heterocyclic compounds, mainly because of their attractive properties, such as (i) exhibition of diverse biological activities,[11] (ii) large Stokes shifts,[12] (iii) flexible functionalization on the parent skeleton, (iv) intramolecular charge transfer (ICT)[13] and (v) acting as a photoinitiator.[14]

Recently, Carlotti and co-workers reported an effective strategy to tailor the photophysics of phenothiazine by utilizing oxygen functionalization on PTZ based push–pull systems.[15] Using the above strategy, they demonstrated that oxidizing the sulfur atom in the PTZ moiety leads to converting intramolecular charge transfer (PTZ derivatives) to a highly efficient emission process (phenothiazine-oxide and dioxide derivatives). In the case of oxygen-functionalized PTZ, the highly fluorescent excited state gets populated due to planar intramolecular charge transfer (PICT). On the other hand, a twisted intramolecular charge transfer (TICT) state is produced upon photoexcitation of the oxygen-free PTZ derivatives, leading to significant fluorescence quenching. They also showed that phenothiazine-5-oxide and phenothiazine-5,5-dioxide acted as weak electron donors relative to phenothiazine for a naphthalimide acceptor. The above exciting strategy of changing TICT to PICT by modulating the electron-donating ability of the phenothiazine chromophore on oxidizing the sulfur atom prompted us to develop phenothiazine as a PRPG.

In this study, we developed for the first time phenothiazine as a fluorescent PRPG for the single and dual release of carboxylic acids and an anticancer drug (valproic acid) on exposure to UV ($\lambda \geq 365$ nm) and visible light ($\lambda \geq 410$ nm) irradiation. Interestingly phenothiazine PRPG showed singlet oxygen generation rather than photorelease on changing the oxidation state of the sulfur atom (S(II) to S(IV)) of the thiazine ring. The difference in the photochemistry between the oxygen-free phenothiazine and oxygen-functionalized phenothiazine PRPGs was investigated and supported by DFT calculations.

Single- and dual-arm phenothiazine based caged esters were synthesized as shown in Scheme 1. First, commercially available 10*H*-phenothiazine was *N*-alkylated and used as a precursor for synthesizing the single- and dual-arm (same and different) caged

[a] *Department of Chemistry, Indian Institute of Technology Kharagpur, Kharagpur 721302, India. E-mail: ndpradeep@chem.iitkgp.ac.in*
[b] *Department of Chemistry, Indian Institute of Technology Kharagpur, Kharagpur 721302, India. E-mail: anoop@chem.iitkgp.ac.in*

† Electronic supplementary information (ESI) available. See DOI: 10.1039/d1cc06950k

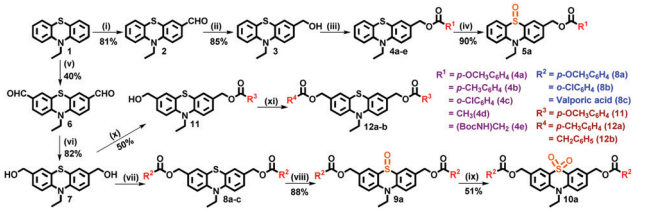

Scheme 1 Synthesis of single- and dual (same and different)-arm caged esters and oxidized caged ester of phenothiazine. Reagents and conditions: $POCl_3$ (1.1 equiv.), DMF, 60 °C, 12 h; (ii) $NaBH_4$, MeOH, r.t., 3 h; (iii) EDC (1 equiv.), R_1COOH (1 equiv.), DMAP, dry DCM, 3 h; (iv) *m*-CPBA, CH_2Cl_2; (v) $POCl_3$ (10 equiv.), DMF, chlorobenzene, 110 °C, 6 h; (vi) $NaBH_4$, MeOH, r.t., 3 h; (vii) EDC (3 equiv.), R_2COOH (3 equiv.), DMAP, dry DCM, 3 h; (viii) *m*-CPBA, CH_2Cl_2; (ix) H_2O_2, acetic acid; (x) EDC (1 equiv.), R_3COOH (1 equiv.), DMAP, dry DCM, 30 min; (xi) EDC (1 equiv.), R_4COOH (1 equiv.), DMAP, dry DCM, 3 h.

esters. To synthesize single-arm caged esters (**4a–e**), first PRPG **3** was obtained by Vilsmeier–Haack formylation of **1** with one equivalent of $POCl_3$, followed by $NaBH_4$ reduction. Then, esterification of **3** with one equivalent of the corresponding carboxylic or amino acids by EDC (1-ethyl-3-(3-dimethylaminopropyl)carbodiimide) coupling generated the desired single-arm caged esters (**4a–e**). For the synthesis of dual-arm (same) caged esters (**8a–c**), PRPG **7** was obtained by Vilsmeier–Haack formylation of **1** with ten equivalents of $POCl_3$, followed by $NaBH_4$ reduction. Compound **7** was then esterified by EDC coupling with three equivalents of the corresponding carboxylic or amino acids to afford the final dual-arm (same) caged esters (**8a–c**). Finally, dual-arm (different) caged esters (**12a** and **12b**) were synthesized, first by esterifying **7** with one equivalent of anisic acid to obtain **11**, and further treatment of **11** with toluic acid (1.0 equiv.) and phenylacetic acid (1.0 equiv.), separately, afforded dual-arm caged esters **12a** and **12b**.

The mono-oxidized phenothiazine (mono-OPTZ) caged ester **5a** was synthesized by oxidizing compound **4a** with *m*-CPBA (*meta*-chloroperoxybenzoic acid). Similarly, the di-oxidized phenothiazine (di-OPTZ) caged ester **10a** was synthesized by oxidizing compound **8a** with *m*-CPBA to form **9a**, and then further oxidation of **9a** with H_2O_2 in the presence of acetic acid afforded compound **10a**. The products obtained in each step were characterized by ^{1}H NMR, ^{13}C NMR, and HRMS (Fig. S1–S30, ESI†).

The absorption and emission spectra of all the phenothiazine-based caged esters (10^{-5} M) were recorded in acetonitrile solution. The absorption spectra of single and dual-arm caged esters **4a** and **8a** exhibited absorption maxima (λ_{abs}) at 307 nm and 308 nm, respectively, which correspond to the localized π–π* transitions (Fig. S31a, ESI†). On the other hand, the absorption spectra of oxidized phenothiazine caged esters **5a** (mono-OPTZ) and **10a** (di-OPTZ) showed absorption maxima at 340 and 335 nm, respectively, which correspond to the n–π* transitions.

In the emission spectrum, the emission maximum of single (**4a**) and dual-arm (**8a**) caged esters were observed at 451 and 456 nm, respectively (Fig. 1a). We found that all single- and dual-arm caged esters showed large Stokes shifts

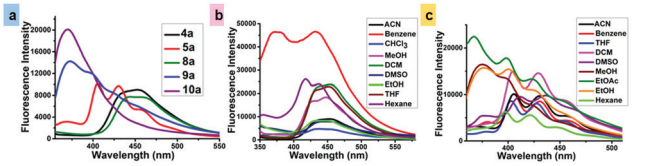

Fig. 1 Emission spectra of (a) single-arm (**4a**), single-arm mono-OPTZ (**5a**), dual-arm (**8a**), dual-arm mono-OPTZ (**9a**) and dual-arm di-OPTZ (**10a**) caged esters in CAN (10^{-5} M), and (b) single-arm (**4a**) and (c) mono-OPTZ (**5a**) caged esters in different solvents (10^{-5} M).

(140 and 148 nm) and exhibited green fluorescence. On the other hand, the emission spectra of oxidized phenothiazine caged esters **5a** (mono-OPTZ) and **10a** (di-OPTZ) exhibited blue-shifted emission maxima at 453 and 350 nm, respectively.

The solvent effects on the absorption and emission spectra were investigated for single-arm caged ester **4a** and mono-oxidized caged ester **5a** (mono-OPTZ). The effects of different solvents on the absorption spectra of **4a** and **5a** were found to be insignificant (Fig. S31b and c, ESI†), whereas we found a pronounced solvent effect on the emission spectra of **4a** and **5a**. It was observed that, in nonpolar solvents (benzene, hexane), the fluorescence intensity of **4a** was comparatively higher, with an emission maximum at 427 nm, whereas in polar solvents (*e.g.*, acetonitrile, tetrahydrofuran, methanol, *etc.*), it exhibited a comparatively lower fluorescence intensity along with a red-shifted emission maximum in the range of 439–460 nm (Fig. 1b). The above results indicate that the excited states of caged esters are stabilized in polar solvents compared to their ground states.

However, the n–π* transition due to the thiocarbonyl group of the oxidized phenothiazine caged ester **5a** shifted towards a shorter wavelength (blue-shift) as the polarity of the solvent was increased (Fig. 1c). The reason is that the non-bonding electrons of oxygen interact strongly (hydrogen bonding) with the hydrogen of polar protic solvents like EtOH, MeOH, EtOAc, *etc.* Hence, the non-bonding electrons are easily promoted to π*, increasing the energy gap between n–π*.[16]

The absorption and emission maxima, Stokes shifts, and fluorescence quantum yields of all the single-(**4a–e**) and dual-arm caged esters (**8a–c**, **12a** and **b**), mono-oxidized caged esters (**5a**, **9a**), and di-oxidized caged ester (**10a**) are summarized in Table S1 (ESI†). The fluorescence quantum yields (Φ_f) of all the caged esters in acetonitrile at room temperature were in the range of $0.026 \leq \Phi_f \leq 0.038$. The fluorescence quantum yields of all the caged esters were calculated using 9, 10-diphenylanthracene as a standard (Φ_f = 0.95 in ethanol).[17]

Considering our main interest in studying the application of phenothiazine as a PRPG, we irradiated all the caged esters (1×10^{-4} M) individually in ACN/H_2O (1 : 1 v/v) using a 125 W medium pressure Hg lamp at two different irradiation wavelengths (≥365 and ≥410 nm). We found that the single- and dual-arm (same and different) caged esters released the corresponding carboxylic acids in high chemical (93–96%) and good photochemical quantum (Φ_p = 0.14–0.20) yields at 365 nm and 410 nm (Table 1). However, in the case of 410 nm, the caged

Table 1 Photochemical data of caged esters (**4a–e**, **5**, **8a–c**, **9a**, **10a**, and **12a** and **b**) in ACN/H_2O (1 : 1 v/v) solvent

	≥365 nm		≥410 nm	
Caged ester	% of deprotection[a]	Quantum yield[b] (Φ_p)	% of deprotection[c]	Quantum yield[d] (Φ_p)
4a	95	0.205	80	0.152
4b	94	0.202	78	0.148
4c	96	0.207	75	0.142
4d	93	0.200	77	0.146
4e	94	0.202	75	0.142
5a	<5	—	<5	—
8a	96	0.207	76	0.144
8b	95	0.205	74	0.140
8c	92	0.201	72	0.139
9a	<5	—	<5	—
10a	<5	—	<5	—
12a	95	0.205	74	0.140
12b	96	0.207	75	0.142

[a] % of deprotection of the caged ester with respect to the initial concentration after 30 min of irradiation time. [b] Photochemical quantum yield at $\lambda \geq 365$ nm (error limit within ±5%). [c] % of deprotection of the caged ester with respect to initial concentration after 240 min of irradiation time. [d] Photochemical quantum yield at $\lambda \geq 410$ nm (error limit within ±5%).

esters required a longer irradiation time to release their corresponding carboxylic acids. The photochemical quantum yield (Φ_p) was calculated using potassium ferrioxalate as an actinometer[18] (see page 39 in the ESI†). Interestingly, we observed insignificant photorelease for the oxidized phenothiazine **5a** (mono-OPTZ) and **10a** (di-OPTZ) caged esters.

The photorelease ability of single-arm caged ester **4a** was monitored by reverse-phase (RP) HPLC at different irradiation intervals (Fig. 2a). The HPLC chromatogram showed a gradual decrease of the peak corresponding to **4a** at the retention time (t_R) 4.65 min, with an increase in irradiation time, indicating the photodecomposition of caged ester **4a**. In addition, we also noted a gradual increase of two new peaks at t_R 2.77 and 3.91 min, which correspond to released carboxylic acids, *i.e.*, *p*-anisic acid and the photoproduct **3**, (10-ethyl-10*H*-phenothiazin-3-yl)methanol, respectively. The corresponding photoproduct (**3**) and released anisic acid were confirmed by injecting authentic samples and isolation and characterization using ^{1}H NMR analysis (Fig. S32, ESI†). Furthermore, we monitored the photorelease of our single-arm caged ester **4a** using fluorescence spectroscopy (Fig. 2b). Also, we monitored the photorelease of dual-arm (same) caged ester **8a** (1×10^{-4} M) in ACN/H_2O (1 : 1 v/v) at 365 nm by ^{1}H NMR (Fig. S33, ESI†) and HRMS (Fig. S34, ESI†) spectroscopy at different irradiation times (0–30 min).

Photoirradiation of dual-arm (different) caged ester **12a** for 20 min resulted in the release of two different carboxylic acids, *i.e.*, *p*-anisic acid and toluic acid, and the formation of photoproduct **7**, which was monitored by HRMS spectroscopy (Fig. S35, ESI†). HRMS analysis found that all the possible intermediates (**11**, **7**) for the stepwise mechanism were present in the reaction mixture along with released carboxylic acids.

The hydrolytic stability of all the caged esters was also tested by keeping them individually in the dark in acetonitrile : water (1 : 1 v/v) for 30 days. We observed only 8–10% decomposition of the caged esters (Table S2, ESI†).

Based on the literature,[19] and photolysis quenching experiments (Fig. S36, ESI†), we suggest a possible stepwise mechanism for the photolysis of phenothiazine caged esters (Scheme 2a). As a representative example, irradiation of dual-arm (different) caged ester **12a** using $\lambda \geq 365$ nm light in aqueous ACN leads to its singlet excited state (S_1), which then undergoes heterolysis of the benzylic C–O bond to produce a tight ion pair. The cation part reacts with the solvent to form photoproduct **11**, and the anion part abstracts a proton to form the released carboxylic acid (*p*-anisic acid). The photoproduct (**11**) formed *in situ* then absorbs light, and gets excited to its singlet state and releases the second carboxylic acid (toluic acid) along with the formation of the final photoproduct (**7**) by following a similar mechanism like the first release.

On the other hand, mono-oxidized phenothiazine caged ester (**9a**) gets excited to its singlet state upon irradiation. It then undergoes ISC to its triplet excited state and transfers its energy to molecular oxygen, resulting in the generation of singlet oxygen (Scheme 2b).

TD-DFT calculations were carried out (for details, see page no. 39–42 in the ESI†) to rationalize the difference in the photochemistry between an oxygen-free phenothiazine caged ester (**4d**) and its oxidized caged ester (mono-OPTZ of **4d**).

We noticed that the electron density of the LUMO of the mono-OPTZ of 4d has more distribution onto the thiocarbonyl group, while the electron density of the LUMO of the single-arm caged ester (**4d**) is dispersed towards the ester group (Fig. S39 and S40, ESI†). Thus, mono-OPTZ of **4d** exhibits a

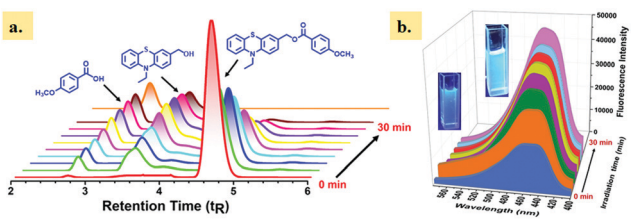

Fig. 2 (a) HPLC profiles for the photolysis of the caged ester **4a** (1×10^{-4} M) in ACN/H_2O (1 : 1 v/v) at different intervals of time (0–30 min). Irradiation wavelength: $\lambda \geq 365$ nm. (b) Change in the fluorescence spectral profiles of **4a** with increasing irradiation time (excitation wavelength 310 nm).

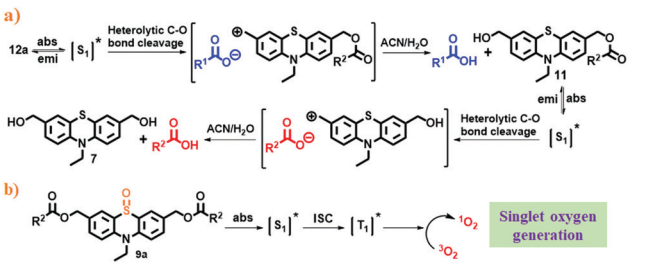

Scheme 2 (a) Possible photorelease mechanism of PTZ caged esters and (b) mechanism for singlet oxygen generation of mono-OPTZ.

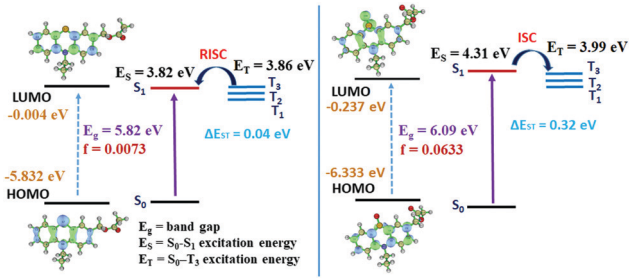

Fig. 3 The energy levels of the singlet and triplet excited states of PTZ and mono-OPTZ caged esters and the exciton decay process after photoexcitation.

relatively larger overlap between the HOMO and LUMO, leading to stronger oscillator strength (*f*) for the S_0–S_1 transition and a larger ΔE_{ST} (Table S3, ESI†). In the case of the single-arm caged ester (**4d**), the energy gap between S_1 and the nearest lower energy triplet state (T_3) is considerably small ($\Delta E_{S1–T3}$ = 0.04 eV); thus, this similar energy level leads to an effective RISC channel from T_3 to S_1 (Fig. 3a).[20] On the other hand, an ISC is expected to be favorable from the S_1 state of the oxidized phenothiazine caged ester of **4d** to T_3 because the $\Delta E_{S1–T3}$ gap is only 0.32 eV (Fig. 3b). Thus, our computations support photocleavage from the singlet excited state and singlet oxygen generation from the triplet excited state. Also, we calculated the energy barriers for photorelease after implementing solvation energies in the SMD model, which are 11.36 kcal mol^{-1} for single-arm caged ester **4d** and 24.49 kcal mol^{-1} for the mono-oxidized caged ester of **4d**. The lower barrier height (13.13 kcal mol^{-1} lower) in the case of **4d** indicates a faster photorelease.

To support the photochemistry of oxidized phenothiazine caged esters occurring from the triplet excited state, we checked their singlet oxygen generation ability by performing DPBF photodegradation. We observed that the decrease in the absorption maximum of DPBF at 415 nm with an increase in irradiation time indicated singlet oxygen generation by our mono-oxidized phenothiazine caged ester (**5a**) and di-oxidized phenothiazine caged ester (**10a**), respectively. The quantum yields for singlet oxygen generation of **5a** (mono-OPTZ) and **10a** (di-OPTZ) were calculated as 0.28 and 0.24, respectively (rose bengal was used as a reference with a Φ_Δ of 0.53)[21] (Fig. S37, ESI†).

In summary, we demonstrated phenothiazine as an efficient PRPG for the single and dual (same and different) release of carboxylic acids from the singlet excited state in the visible wavelength region. The phenothiazine caged esters exhibited green fluorescence with a large Stokes shift. Interestingly the oxidized phenothiazine caged esters generated singlet oxygen rather than photorelease due to the thiocarbonyl group resulting in efficient ISC to its triplet excited state, supported by DFT calculations.

We thank DST SERB (Grant No. DIA/2018/000019) for the financial support and DST (SR/FST/CSII-026/2013) for the 400 MHz NMR spectrometer. We acknowledge the Supercomputing Facility "PARAM Shakti" at IIT Kharagpur established under National Supercomputing Mission (NSM), Government of India. M. Ojha is thankful to UGC-New Delhi for the fellowship and M. Banerjee acknowledges IIT Kharagpur for the fellowship.

Conflicts of interest

There are no conflicts to declare.

References

1 (*a*) R. Weinstain, T. Slanina, D. Kand and P. Klán, *Chem. Rev.*, 2020, **120**, 13135; (*b*) D. Kand, P. Liu, M. X. Navarro, L. J. Fischer, L. R. Noori, D. F. Morvinski, A. H. Winter, E. W. Miller and R. Weinstain, *J. Am. Chem. Soc.*, 2020, **142**, 4970.
2 S. S. Agasti, A. Chompoosor, C. C. You, P. Ghosh, C. K. Kim and V. M. Rotello, *J. Am. Chem. Soc.*, 2009, **131**, 5728.
3 N. C. Fan, F. Y. Chenge, J. A. Ho and C. S. Yeh, *Angew. Chem., Int. Ed.*, 2012, **51**, 8806.
4 C. M. J. Hu and L. Zhang, *Biochem. Pharmacol.*, 2012, **83**, 1104.
5 Y. Li, T. Thambi and D. S. Lee, *Adv. Healthcare Mater.*, 2018, **7**, 1700886.
6 Y. Venkatesh, H. K. Srivastava, S. Bhattacharya, M. Mehra, P. K. Datta, S. Bandyopadhyay and N. D. P. Singh, *Org. Lett.*, 2018, **20**, 2241.
7 P. T. Wong, S. Tang, J. Cannon, J. Mukherjee, D. Isham, K. Gam, M. Payne, S. A. Yanik, J. R. Baker and S. K. Choi, *ChemBioChem*, 2017, **18**, 126.
8 A. Chaudhuri, Y. Venkatesh, K. K. Behara and N. D. P. Singh, *Org. Lett.*, 2017, **19**, 1598.
9 A. Sikder, M. Banerjee, T. Singha, S. Mondal, P. K. Datta, A. Anoop and N. D. P. Singh, *Org. Lett.*, 2020, **22**, 6998.
10 (*a*) Y. Hua, S. Chang, D. Huang, X. Zhou, X. Zhu, J. Zhao, T. Chen, W. Y. Wong and W. K. Wong, *Chem. Mater.*, 2013, **25**, 2146; (*b*) Y. Lu, H. Song, X. Li, H. Ågren, Q. Liu, J. Zhang, X. Zhang and Y. Xie, *ACS Appl. Mater. Interfaces*, 2019, **11**, 5046.
11 (*a*) B. Varga, Á. Csonka, A. Csonka, J. Molnár, L. Amaral and G. Spengler, *Anticancer Res.*, 2017, **37**, 5983; (*b*) K. Pluta, M. Jeleń, B. M. Młodawska, M. Zimecki, J. Artym, M. Kocięba and E. Zaczyńska, *Eur. J. Med. Chem.*, 2017, **138**, 774.
12 (*a*) J. Gai, C. Chen, J. Huang, J. Sheng, W. Chen and X. Song, *Tetrahedron Lett.*, 2020, **61**, 152038; (*b*) X.-Y. Qi, S.-J. Liu, Y.-Q. Hao, J.-W. Sun and S. Chen, *Spectrochim. Acta, Part A*, 2020, **227**, 117675.
13 W. Qiu, X. Cai, M. Li, L. Wang, Y. He, W. Xie, Z. Chen, M. Liua and S.-J. Su, *J. Mater. Chem. C*, 2021, **9**, 1378.
14 X. Ma, R. Gu, L. Yu, W. Han, J. Li, X. Li and T. Wang, *Polym. Chem.*, 2017, **8**, 6134.
15 Y. Rout, C. Montanari, E. Pasciucco, R. Misra and B. Carlotti, *J. Am. Chem. Soc.*, 2021, **143**, 9933.
16 A. I. Adeogun, N. W. Odozi, N. O. Obiegbedi and O. S. Bello, *Afr. J. Biotechnol.*, 2008, **7**, 2736.
17 J. V. Morris, M. A. Mahaney and J. R. Huberr, *J. Phys. Chem.*, 1976, **80**, 969.
18 J. N. Dema, W. D. Bowman, E. F. Zalewsk and R. A. Velapold, *J. Phys. Chem.*, 1981, **85**, 2766.
19 R. Schmidt, D. Geissler, V. Hagen and J. Bendig, *J. Phys. Chem. A*, 2007, **111**, 5768.
20 D. Hu, L. Yao, B. Yang and Y. Ma, *Philos. Trans. R. Soc., A*, 2015, **373**, 0318.
21 N. E. Elezcanoa, V. M. Martínez, E. P. Cabrerab, C. F. A. G. Duránb, I. L. Arbeloaa and S. Lacombe, *RSC Adv.*, 2016, **6**, 41991.